

Measuring the Conformational Stability of a Protein by Hydrogen Exchange

Beatrice M. P. Huyghues-Despointes, C. Nick Pace,
S. Walter Englander, and J. Martin Scholtz

1. Introduction

Measuring the conformational stability of a protein is one key to solving the protein folding problem. It is also of practical importance for answering questions such as these:

1. How stable is a protein under physiological conditions?
2. How does the stability depend on temperature, pH, and salt concentration?
3. Can the stability be increased by osmolytes?
4. Can the stability be increased by ligands that bind the native state?
5. Does an amino-acid substitution increase or decrease the stability?

Thus, reliable techniques for measuring the conformational stability of proteins are essential. In this chapter, we briefly review the traditional methods that have been used to measure the conformational stability of a protein, and describe in more detail how the conformational stability can be measured using hydrogen-exchange rates as monitored by nuclear magnetic resonance (NMR).

2. Determining Protein Conformational Stability

The conformational stability is defined as the free-energy change of the unfolding reaction, $F \rightleftharpoons U$, under ambient conditions (generally around room temperature and neutral pH): $\Delta G_U = G_U - G_F$. It can be evaluated using the relationship $\Delta G_U = -RT \ln K_U$, where K_U is the equilibrium constant of the unfolding reaction. Measuring the conformational stability and changes in stability of proteins that differ slightly in structure helps to define the forces that determine the conformations of proteins and optimize their stabilities. The stability of the folded conformation is a delicate balance between compensating forces: favorable hydrophobic, van der Waals, and hydrogen-bonding interactions and unfavorable conformational entropy. The result is that the folded protein is only marginally stable, generally 5–15 kcal/mol under native conditions (**1**).

A protein exists predominantly in the folded conformation under ambient conditions, but rarely, as dictated by the Boltzmann relationship, $P_F/F = e^{-\Delta G_U/RT}$, this conformation will unfold to partially unfolded or completely unfolded higher energy conformations (*see Fig. 1*). As a result, it is difficult to detect the unfolded conformations and to directly measure K_U under native conditions. In the traditional methods, the conformational stability is extrapolated from stabilities obtained under denatured conditions, while in the hydrogen-exchange experiments, conformational stability is determined directly under native conditions.

2.1. Traditional Methods: Solvent and Thermal Denaturation

The most common way to estimate the conformational stability of a protein is to tilt the equilibrium to conditions where the folded and unfolded states are almost equally populated, measure the stability, and extrapolate to obtain the stability under native conditions. Traditional methods of measuring ΔG_U are solvent (urea or guanidinium chloride [GdmCl] or thermal denaturation (*see Fig. 2*) (**2**). Solvent denaturation curves are generally analyzed using the linear extrapolation method (LEM):

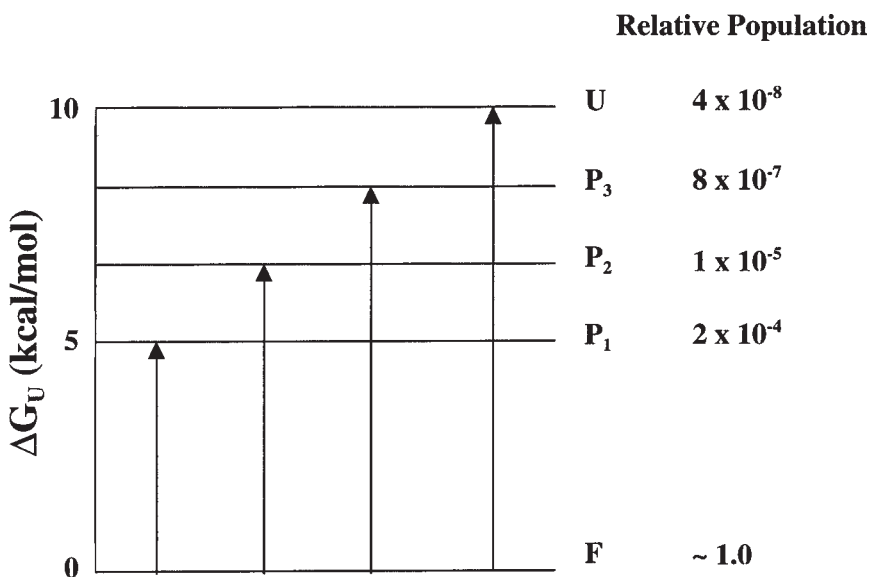


Fig. 1. An energy manifold of states at 25°C for a protein having $\Delta G_U = 10$ kcal/mol, including the folded (F) and unfolded (U), and partially unfolded states (P_i).

$$\Delta G = \Delta G_U(\text{H}_2\text{O}) - m[\text{denaturant}] \quad (1)$$

where m is a measure of the dependence of ΔG on denaturant, and $\Delta G_U(\text{H}_2\text{O})$ is an estimate of the conformational stability that assumes that the linear dependence of ΔG on denaturant observed in the transition region continues to 0 M denaturant. Thermal denaturation experiments yield the melting temperature, T_m , the enthalpy change at T_m , ΔH_m , and the heat-capacity change, ΔC_p , which can then be used to calculate ΔG_U at any temperature T , $\Delta G_U(T)$, with the Gibbs-Helmholtz equation:

$$\Delta G_U(T) = \Delta H_m(1 - T/T_m) + \Delta C_p[T - T_m - T \ln(T/T_m)] \quad (2)$$

The equilibrium between the folded and unfolded states can be monitored by calorimetry (3), or by using spectroscopic techniques such as UV absorbance spectroscopy, fluorescence, and circular dichroism that monitor the changes in conformational states of a protein (4).

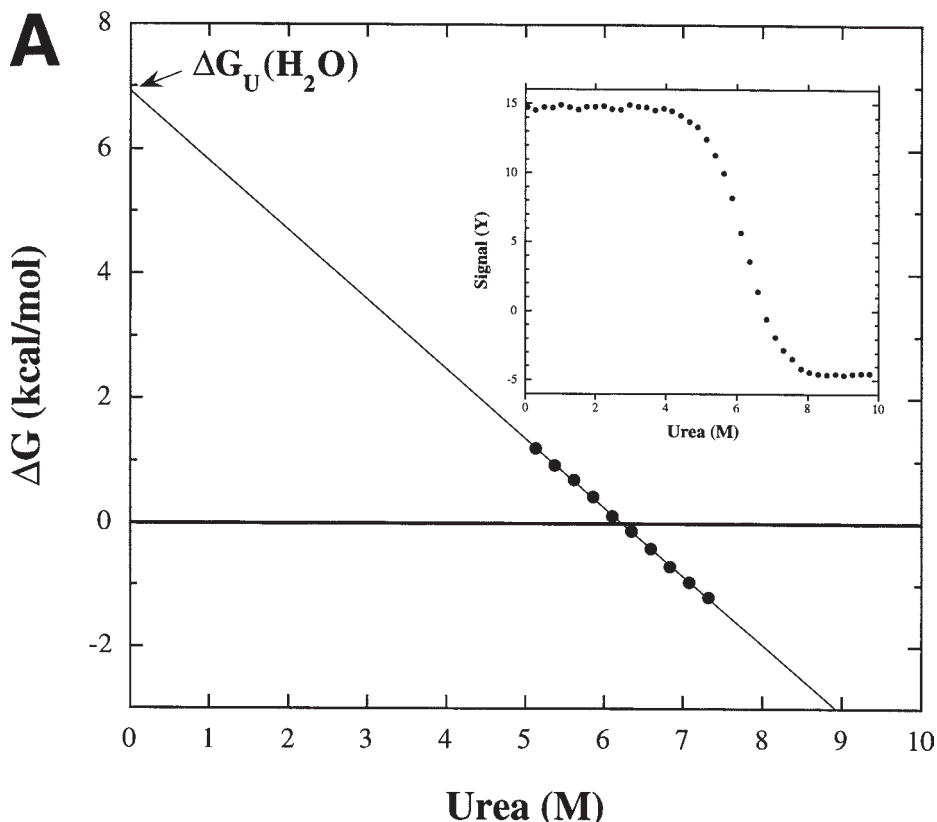


Fig. 2. (A) The inset shows a typical urea unfolding curve for a small monomeric protein. The data in the transition region can be extrapolated to determine $\Delta G_U(\text{H}_2\text{O})$ using the LEM (Eq. 1).

There are several problems with these techniques. Traditional methods are usually unable to detect unfolded forms under ambient conditions because their concentrations are far too low. These methods for determining the conformational stability also depend on some basic limiting assumptions. First, they require that the folding transition of a protein be fully reversible, with a known and finite number of observable states. Above, we show the simplest example—a two-state mechanism—but the models can be expanded for analysis of multimeric protein systems or proteins that fold by mechanisms with intermediate states (5).

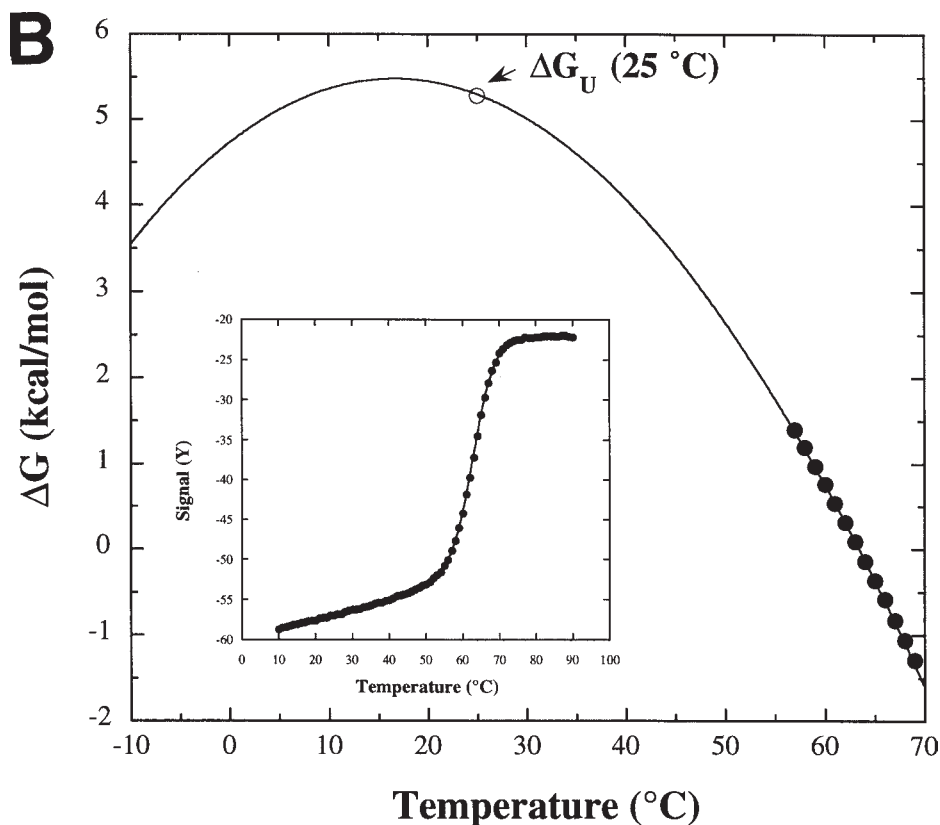


Fig. 2. (continued) **(B)** The inset shows a typical thermal unfolding curve for a small monomeric protein. The data in the transition region of a thermal unfolding curve can be extrapolated to obtain ΔG_U at a desired reference temperature such as 25°C using the Gibbs-Helmholtz relationship (**Eq. 2**).

Second, both methods require a long extrapolation from unfolding to ambient conditions. The LEM assumes that the dependence on denaturant can be extended linearly to the absence of denaturant. This may not always occur, especially for GdmCl, a salt that can alter the stability of a protein at low denaturant concentrations through an ionic strength effect (*see ref. 6* and references therein). For thermal denaturation, the extrapolation from higher temperatures to ambient temperatures requires an accurate value of ΔC_p . At best, ΔC_p can be measured to approx $\pm 10\%$ with calorimetry.

Finally, the unfolded states in denaturant or at high temperatures may not be thermodynamically equivalent to the unfolded states under ambient conditions.

2.2. The New Method: Hydrogen Exchange

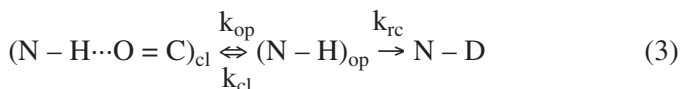
When a protein is placed in D₂O, amide hydrogens in the protein begin to exchange with deuterium. The rate of exchange of an amide depends on its environment in the protein. An unprotected amide exchanges readily with the solvent. In contrast, an amide that is shielded from solvent by burial and/or hydrogen bonding can exchange only a small fraction of time when it unfolds to a higher energy conformation that is exposed to solvent. The exchange of a backbone amide proton can occur by local fluctuations, such as the breaking of only a few hydrogen bonds, or by a larger global unfolding event. The result is that exchange rates of amide protons in a protein vary widely, providing a clear view of the higher energy unfolded states under native conditions (*see Fig. 1*) (7).

We describe here a NMR technique that identifies amides that exchange from the globally unfolded protein. Hydrogen-exchange measurements under fully native conditions can provide a direct estimate of the conformational stability of a protein without having to drive the protein through its macroscopic unfolding transition. This technique, which can measure the conformational stability of a protein, may not be possible by traditional methods because folding is irreversible or does not approach a two- or three-state folding mechanism.

3. The Hydrogen-Exchange Process

3.1. The Rate Constants Governing Exchange

The exchange process can be described using a general two-step model:



where k_{op} and k_{cl} are the rate constants for structural opening and closing, respectively, and $(N-H)_{op}$ is the open form that exchanges with solvent at the intrinsic rate constant k_{rc} , where rc stands for random coil (8,9). The second step is written as an irreversible reaction because of exchange with a vast excess of solvent D_2O . The measurable rate constant $k_{ex} = k_{op}k_{rc}/(k_{op} + k_{cl} + k_{rc})$. If the protein is present mainly in the open form ($k_{op} \gg k_{cl}$), $k_{ex} = k_{rc}$. If the protein is present mainly in the closed form ($k_{op} \ll k_{cl}$), then two mechanisms could potentially occur, depending on conditions, either as two distinct processes or in combination (10,11).

The EX1 exchange conditions (monomolecular exchange) exist when $k_{cl} \ll k_{rc}$, so that $k_{ex} = k_{op}$. The EX2 exchange conditions (bimolecular exchange) exist when $k_{cl} \gg k_{rc}$, so that $k_{ex} = K_{op}k_{rc}$, where K_{op} is the equilibrium constant for structural opening (k_{op}/k_{cl}). Thus, under EX2 conditions, the free energy of structural opening is given by:

$$\Delta G_{HX} = -RT \ln (k_{ex}/k_{rc}). \quad (4)$$

One expects a subset of the ΔG_{HX} values to generally represent the complete unfolding reaction; thus, it has been proposed that the average of the three largest ΔG_{HX} values calculated using Eq. 4 provides a reasonable estimate of the conformational stability of a protein (12).

3.2. The k_{rc} Values from Model Peptides

Exchange from the open form depends on k_{rc} . The k_{rc} value can be approximated by the chemical exchange rates of amide groups in nonstructured peptides. The rate constants in short (1–5 amino acids long) peptides and in poly-DL-alanine (PDLA) have been measured (9,13,14). The results show that exchange-rate constants of backbone amide protons are dependent on pH, temperature, identity of neighboring side-chain residues in the sequence, solvent isotope effects, and small ionic strength effects. The exchange-rate constants for alanine-based reference peptides at low ionic strengths and 20°C are shown in Table 1.

Table 1
H to D Exchange Rate Constants
for Alanine-Based Models at 293 K^a

Model	log k_A (M ⁻¹ min ⁻¹)	log k_B (M ⁻¹ min ⁻¹)	log k_W (min ⁻¹)
N-Ac-A-A-A-N'MA ^b	2.04	10.36	-1.5
PDLA ^c	1.62	10.05	-1.5

^aThese values are specific for NH to ND exchange under normal low salt conditions, using $pD = pH^* + 0.4$ and $pK_a = 15.05$ for the D₂O at 20°C. These data are from **Table 3** in Bai et al. (9).

^bL-alanine tripeptide blocked by N-acetyl at N-terminus and N'-methylamide at C-terminus.

^cpoly-DL-alanine.

The NH to ND chemical exchange process can be acid (k_H), base (k_{OH}), or water catalyzed (k_W), yet the latter generally makes only a negligible contribution:

$$K_{rc} = k_A 10^{-pD} + k_B 10^{[pD - pK_D]} + k_W \quad (5)$$

where pD is the corrected reading in D₂O (*see* below) and pK_D is the molar ionization constant of D₂O. The rate of exchange of a backbone amide reaches a minimum near $pH \sim 3$ and increases substantially at both pH extremes, by a factor of 10 per pD unit (**Eq. 5**). The chemical exchange rate of amide proton of residue i in a sequence is affected by its own side chain and the side chain of residue $i-1$. For example, we show in **Fig. 3** for two dipeptide sequences in RNase T1 that k_{rc} can vary by 20-fold. **Fig. 3** also illustrates the dependence of k_{rc} on pH .

The intrinsic rate of exchange can also change with temperature. The rate constant for the acid-catalyzed exchange can be modified by:

$$k_A(T) = k_A(293 \text{ K}) e^{(-E_a[1/T - 1/293]/R)} \quad (6)$$

where the activation energy, $E_a(k_H) = 14$ kcal/mol. Analogous expressions can be made for the base- and water-catalyzed exchange in **Eq. 5**, where $E_a(k_{OH}) = 17$ kcal/mol, and $E_a(k_W) = 19$ kcal/mol,

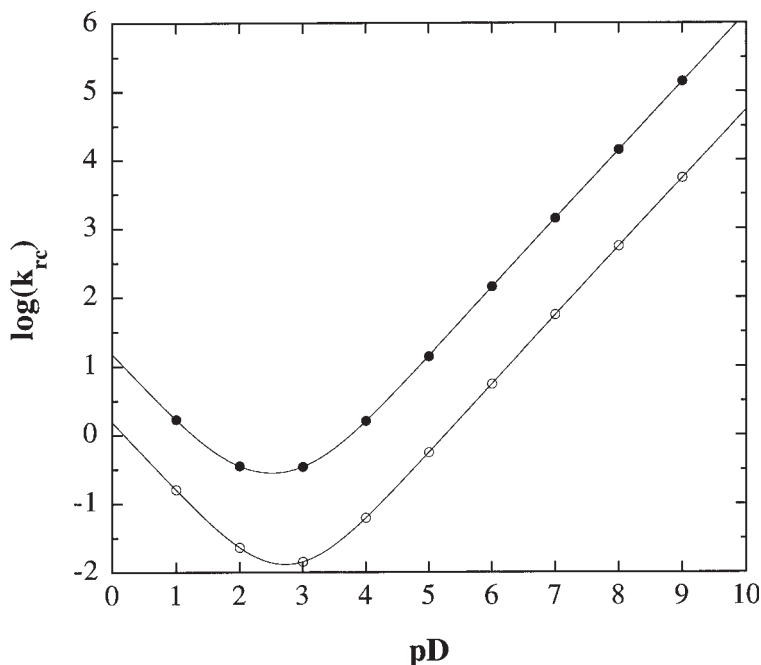


Fig. 3. Log (k_{rc}) vs pD for two dipeptide sequences, $-Gly71-Ser72-$ (●) and $-Val89-Ile90-$ (○), in RNase T1 using k_{rc} values from Bai et al. (9). Curves represent the data fit to Eq. 5.

respectively. To determine ΔG_{HX} in a protein, the exchange-rate constants of random coil peptides can be used to predict k_{rc} values for every residue at a particular pH and temperature. (See the spreadsheet at <ftp://hxiris.med.upenn.edu/HX/> to do it for your favorite protein).

3.3. EX1 and EX2 Conditions

The exchange process for a globally exchanging residue must be EX2 in order to determine the conformational stability of the protein by the hydrogen-exchange method. Three methods are used to establish whether an amide proton exchanges by an EX1 or EX2 mechanism (15). The simplest method is to plot $\log k_{ex}$ for several

amide protons at two different pH values above pH 4.0 and in a pH region where the stability of the protein changes as little as possible. For the EX2 process, the hydrogen-exchange rates for each NH group should change by 10-fold, with a one-unit change in pH, showing the expected pH dependence on k_{rc} (see **Fig. 3**). In the EX1 process, k_{ex} depends only on k_{op} , which is likely to be less dependent on pH. As a result, we would observe little to no rate variation with pH in the EX1 regime.

Another test of EX2 vs EX1 kinetics uses the nuclear Overhauser effect (NOE) (**15–18**). We can measure a decrease in the NOE intensity between two adjoining residues as hydrogen-exchange progresses. In the EX1 limit, two amide protons will exchange at the same rate, so that the decay rate of the NOE will be equal to the exchange rate of a single amide proton. Conversely, in the EX2 limit, two amide protons will exchange independently and often with different chemical exchange rates. Therefore, the decay rate of the NOE will be the sum of the exchange rates of the two adjoining amide protons. This method is often arduous, and errors in measurement can be significant (**15**).

A third method is simply to compare the ΔG_{HX} values for neighboring amide groups with their corresponding k_{rc} values. In an EX2 process, the same ΔG_{HX} values are likely to have widely different k_{rc} values. The opposite holds true for the EX1 process.

3.4. ΔG_{HX} for Measurable Amide Protons

The hydrogen-exchange technique provides a glimpse into the distribution of unfolded conformations at native conditions. Exchange of an amide proton with solvent deuterium occurs only through exchange-competent, higher-energy forms. The amide groups that are most protected from exchange have the largest stabilities and may be limited to exchange only from the fully unfolded state (“global”). Residues with intermediate and low stabilities (or protection) exchange by either fluctuations in the native state (“local”) or by partial unfolding (“subglobal”). Here, we describe an NMR technique that identifies only the global-exchanging resi-

dues. Monitoring hydrogen exchange in response to external perturbants, such as temperature, solvent denaturants (19–25) or pressure (26), can help to decipher the exchange processes of local and subglobal amide groups.

Hydrogen-exchange studies with mutant proteins have also been performed where the change in stability upon mutation, $\Delta\Delta G_{\text{HX}}$, can be obtained by:

$$\Delta\Delta G_{\text{HX}} = (\Delta G_{\text{HX}})_{\text{WT}} - (\Delta G_{\text{HX}})_{\text{mutant}} = -RT \ln(k_{\text{ex}})_{\text{WT}} / (k_{\text{ex}})_{\text{mutant}} \quad (7)$$

The k_{rc} values for all residues cancel in **Eq. 7**, except for the mutation site and the residue C-terminal to the site of the mutation. The residues that exchange by global unfolding will have $\Delta\Delta G_{\text{HX}}$ values similar to the values determined by the traditional methods. Unfortunately, there can also be nonglobal residues that have $\Delta\Delta G_{\text{HX}}$ values equal to or even greater than $\Delta\Delta G_{\text{U}}$ (27). Additional experiments that monitor the effect of an external perturbant on the hydrogen-exchange stabilities are required to decipher the stability patterns of nonglobal residues. As a result, hydrogen-exchange studies with mutant proteins cannot in themselves determine the residues that unfold globally.

4. The NMR Experiment

4.1. Establishing Experimental Conditions

The hydrogen-exchange experiment by NMR entails monitoring the decay of individual proton resonances over time as they exchange with solvent deuterium. We assume that standard sequential NMR assignment techniques have been used to identify amide resonances that persist upon the addition of deuterium. Normally, the overcrowding of proton resonances in a protein limits the usefulness of 1D proton spectra. Instead, popular two-dimensional experiments have been used, such as proton-detected magnitude-mode Correlation Spectroscopy (COSY), and more recently, inverse-detected ^{15}N Heteronuclear Single Quantum Coherence (HSQC). For hydrogen exchange, the HSQC experiment provides

better resolution when observing the exchange of many exchangeable backbone amide groups in larger proteins (15–25 kDa), and in most cases, HSQC spectra can be acquired in less time. The limitations to the heteronuclear approach are that the protein must be uniformly labeled with ^{15}N —usually by overproduction in bacteria, grown in minimal media where yields are generally reduced. ^{15}N -labeled precursors are expensive (although prices are steadily decreasing), and some degree of technical expertise of the NMR hardware and software is required.

A positive attribute of measuring the conformational stability by hydrogen exchange is that only the exchange rates of the most stable NH groups must be determined. This simplifies assignments and in most cases, simple 1D-proton spectra may be taken to collect the data. The most stable amide resonances are usually the ones that persist over the longest time. Most other resonances disappear from the spectra by the time the most stable amide protons begin to exchange. However, caution must be exercised, because the most stable residue may not always be the slowest exchanging residue. As shown in **Fig. 3** and **Eq. 4**, k_{rc} varies with sequence and can affect the exchange time and the stability value of a residue. To be safe, the exchange of at least the 10 slowest exchanging amide protons should be monitored.

It is important to establish the best pH and temperature conditions to monitor the decay of the most stable NH groups. The random coil rate of each residue and the stability of the protein play important roles in determining the best experimental conditions. For example, RNase T1 has a bell-shaped stability vs pH profile with a stability maximum of ~ 13 kcal/mol near pH 5.0 and 25°C in D_2O (28). If we monitor exchange at these conditions, the most stable residues would not exchange for over 100 years! As a result, experimental conditions must be chosen to allow the data to be collected in a reasonable amount of time. If we raise the pH or increase the temperature for RNase T1, the exchange is considerably faster (pD 7.7, 25°C —3–6 months, and 40°C —days). Another method to reduce the time of exchange at a desired experimental condition is

to perform measurements at two or more concentrations of denaturant where the protein is still fully folded (the pretransition region of **Fig. 2A**), and extrapolate to the ΔG_{HX} in the absence of denaturant using **Eq. 1**. With both these techniques, it is important to test whether the exchange process is still in the EX2 regime. Conversely, if a protein is marginally stable, the temperature or the pH can be decreased in order to observe the decay of the most stable amide protons. Stabilities in a range of 4–10 kcal/mol can be measured using the hydrogen-exchange technique described here. A good starting point is to perform one-dimensional hydrogen-exchange experiments at several different conditions. If exchange is too slow or too fast, adjust the conditions until the most stable residues exchange in a reasonable amount of time and by the EX2 process.

4.2. Sample Preparation

NMR samples are prepared by dissolving the protein in an H_2O buffered solution. A 0.5–2 mM solution of protein (0.5–1.0 mL) is required. The one-dimensional experiment needs less protein than the two-dimensional experiment. The pH of this solution should be equal to the desired pD of the deuterated NMR sample. The pD of a solution in D_2O is the pH meter reading (pH^*) plus 0.4 ($\text{pD} = \text{pH}^* + 0.4$) (**29**). Measuring the pH^* of a deuterated solution is performed as follows:

1. Use appropriate standard pH buffers in H_2O to calibrate your pH meter, considering the effect of temperature on the buffers.
2. Allow the electrode to soak in D_2O until the meter reading is steady (5–10 min).
3. Read the pH meter value of your sample (pH^*) and make the appropriate correction for pD.

It is important to ensure that the protein sample is fully dissolved and at equilibrium before exchanging the H_2O for D_2O . If any particulate remains, centrifuge the sample and place the solution in a fresh Eppendorf tube. Buffers that are silent in the NMR experiment

should be used—such as phosphate that lacks protons or one such as acetate, which can be purchased inexpensively in a deuterated form. The sample can be exchanged into D_2O by using a spin-column (Isolab, Inc.). The spin-column approach can be performed as follows:

1. Swell 1 g of G-25 resin in 10 mL of D_2O for a minimum of 3 h.
2. Remove fines by stirring and replacing with an equal vol of fresh liquid (2–3 times), pour deuterated buffer onto the resin for the last volume exchange, and equilibrate for 10 min.
3. Pour the resin into the spin column (~3 mL) and wash the resin several times with 0.5–1.0 mL volumes of deuterated buffer, by spinning the column in a swinging bucket benchtop centrifuge at ~1000g for 1-min intervals. Be sure to balance the rotor by using a dummy column with resin in it.
4. Exchange the protein solution in H_2O with D_2O by loading the sample in H_2O onto the column and spinning the column for a 1-min interval. The number of spins and the vol of sample added can be adjusted so that a final vol of recovered sample is ~ 0.7 mL and protein yield is 80–90%. (After the experiment, if the protein is valuable, one can rescue the rest of the protein left on the column by rinsing with several volumes of buffer.)
5. Immediately after exchange, transfer the solution to a NMR tube, and quickly adjust the pH^* of your solution with NaOD or DCl if it has changed. The pH^* in the NMR tube can be measured using a long, thin electrode from Ingold.
6. Place the sample in the NMR spectrometer with the probe temperature set at the appropriate temperature, and acquire a data set.
7. Measure the pH^* of the sample after the conclusion of the NMR data set.

4.3. NMR Data and Analysis

NMR spectra must be collected over time. The NMR sample should be equilibrated in a water bath at the appropriate temperature if the NMR data are not acquired in a single time period. The spectra are processed by standard processing programs. The peak intensities for each residue can be measured either by peak heights (one-dimensional experiments) or by volume integration (two-dimensional

crosspeaks). These measurements can fit to a single exponential function, $A = A_0[e^{(-k_{\text{ex}}t)}] + C$, where C is the baseline noise of a particular spectra caused by residual water in the sample. With partial or completely overlapping peaks, the exchange data may be fit to a sum of exponentials, especially if rates for amide protons differ by more than approximately threefold. The exchange rate should be measured only after the peak is approx 50% exchanged. The errors in stability are the largest for residues whose hydrogen exchange rates are either very fast or very slow. For a typical exchange experiment, two fold variations in the rate only affect ΔG_{HX} by 0.4 kcal/mol.

5. Comparison of ΔG_{HX} and ΔG_{U}

The measured hydrogen-exchange stabilities of the most stable residues are generally higher than the conformational stabilities measured by urea and thermal denaturation, as shown for a variety of proteins in **Table 2**. There are two main reasons for the discrepancies: solvent isotope effects and proline isomerization effects.

5.1. Solvent Isotope Effect

To compare denaturation and hydrogen-exchange experiments, the traditional techniques must be performed in D_2O . At this time, we cannot predict whether a protein will be more or less stable in D_2O than in H_2O , since many factors affect the solvent isotope effect of a protein (30). We have ample evidence from data by Makhatadze et al. (31), the review by Oas and Toone (30), and Huyghues-Despointes et al. (12) that ΔG_{U} values can differ by $\pm 0\text{--}2$ kcal/mol in H_2O compared to D_2O , and the difference may be dependent on pH.

5.2. Proline Isomerization Effect

Denatured states at native-state conditions in the hydrogen-exchange experiments differ from denatured states under equilibrium unfolding conditions in traditional experiments. Most peptide bonds in a folded protein are in a *trans* conformation. Only 0.03%

Table 2
Comparison of Conformational Stabilities Measured
by Hydrogen Exchange and Traditional Methods^a

Protein	No. of Proline <i>cis</i>	Residues <i>trans</i>	ΔG_{HX} (kcal/ mol)	ΔG_{HX}^* (kcal/ mol)	$\Delta G_{\text{U}}(\text{D}_2\text{O})$ (kcal/mol)
RNase T1	2	2	10.7	8.2	7.9 (UDC) 8.0 (TDC)
A21G ^b				7.2	7.1 (UDC)
G23A ^b				7.1	7.0 (UDC)
A21G+G23A ^b				6.3	6.0 (UDC)
RNase A	2	2			
Mayo and Baldwin			(10.2)	7.8	7.7 (DSC)
Wang et al.			10.3	8.0	8.1 (DSC)
Neira et al.			9.4	7.0	7.0 (DSC)
barnase	0	3	8.3	8.1	8.3 (DSC)
CI2	0	5	7.6	7.1	7.0 (GDC)
434 cro	0	2	4.0	3.9	3.7 (UDC)
apocytochrome b ₅₆₂	0	4	5.5	5.3	5.0 (DSC) 3.3 (GDC)
cytochrome c (equine)	0	4			
Bai et al.			(9.3)	9.0	9.1 (DSC)
Foord and Leatherbarrow			6.4	6.1	6.1 (DSC)
cytochrome c (yeast)	0	4	6.8	6.5	6.4 (TDC)
HEWL	0	2	12.4	12.2	11.7 (DSC)
NTL9	0	1	4.8	4.7	4.7 (TDC+UDC)
OMTKY3	1	2	8.2	7.2	7.2 (DSC)
PPL	0	0	(6.9)	6.9	6.7 (TDC) 4.9 (GDC)
HPr (<i>Escherichia coli</i>)	0	2	5.8	5.7	4.7 (UDC)
src SH3 domain	0	2	6.2	6.1	4.7 (TDC) 4.7 (GDC)
Barstar	0	2	6.2	6.0	5.0 (GDC)
RNase H* (<i>Escherichia coli</i>)	1	4	(10.9)	9.3	9.9 (GDC)
RNase H (<i>T. thermophilus</i>)	1	11	(15.8)	13.8	13.3 (GDC)
CTXIII ^c		5	6.6	6.3	6.0 (GDC)
RNase A ^d	2	2	11.8	9.6	9.2 (DSC)
RNase Sa ^e	1	5	8.9	7.3	7.5 (GDC)
T4 lysozyme ^f		3	(17.7)	17.5	16.0 (GDC)
SNase ^g	2	4			
Unligated			6.4	4.4	6.1 (UDC)
Ligated (Ca ²⁺ and pdTp)			8.2	6.2	7.4 (UDC)
SNase ^h (Unligated)	2	4	~ 6.4	~ 4.5	4.0 (GDC)
E75A			~ 4.4	~ 2.5	2.0 (GDC)

(Continued)

Table 2 (continued)

Protein	No. of Proline <i>cis</i>	Residues <i>trans</i>	ΔG_{HX} (kcal/ mol)	ΔG_{HX}^* (kcal/ mol)	$\Delta G_{\text{U}}(\text{D}_2\text{O})$ (kcal/mol)
M26G			~ 4.4	~ 2.5	2.3 (GDC)
D77A			~ 4.1	~ 2.2	3.1 (GDC)
V23A			~ 3.4	~ 1.5	2.2 (GDC)

^aUnless otherwise indicated below, the specific conditions for each protein are given in the footnote to **Table 1** in Huyghues-Despointes et al. (12). ΔG_{HX} is the average ΔG_{HX} value of the three most stable residues. ΔG_{HX} values in parentheses were estimated by extrapolation of hydrogen exchange stabilities at higher denaturant concentrations (15). $\Delta G_{\text{HX}}^* = \Delta G_{\text{HX}} - \Sigma \Delta G_{\text{pro}}$. $\Delta G_{\text{U}}(\text{D}_2\text{O})$ is measured by the LEM (Eq. 1) using urea (UDC) or GdmCl (GDC) denaturation curves, or by the Gibbs-Helmholtz equation (Eq. 2) using thermal denaturation curves (TDC) or differential scanning calorimetry (DSC).

^bpD = 7.4 and 25°C (27).

^cCardiotoxin analog III. pD = 3.6 and 25°C (39).

^dpD = 6.4 and 25°C (40).

^epD = 5.9 and 30°C (D. Laurents, J.M. Pérez-Cañadillas, J. Santoro, M. Rico, D. Schell, C. N. Pace, and M. Bruix, personal communication).

^fpD = 6.0 and 25°C (41).

^gpD = 5.9 and 37°C (42 and references therein). Lys-Pro117 is 91% *cis* and His-Pro47 is 9% *cis* in the folded unligated protein. Lys-Pro117 is greater than 98% *cis* in the folded ligated protein.

^hpD = 5.6 and 25°C (43).

of the nonproline bonds and 5.2% of the proline bonds are in a *cis* conformation in folded proteins (32). Conversely, an unfolded protein at equilibrium has nonproline bonds exclusively in the *trans* conformation and 6–38% of the proline bonds in the *cis* conformation, depending on the identity of the residue preceding proline. The latter values are based on data by Reimer et al. (33) on capped pentapeptides with 20 different amino acids at the Xaa-Pro position (see **Table 3**).

Transiently unfolded states under native conditions in the hydrogen-exchange experiments have the proline bonds in the same conformation as in the folded protein because the rate of refolding and hydrogen exchange is often much faster than the rate of proline

Table 3
Proline Isomerization Based on Ac-Ala-Xaa-Pro-Ala-Lys-NH₂^a

Xaa	% <i>cis</i> ^b	K _{Pro} ^{Uc}	RT ln (1+K _{Pro} ^U) ^d	RT ln (1 + 1/K _{Pro} ^U) ^e
Pro	6.0	15.67	1.67	0.037
Lys	6.8	13.71	1.59	0.042
Arg	7.2	12.89	1.56	0.044
Asp	7.3	12.70	1.55	0.045
Ala	7.7	12.00	1.52	0.047
Cys	8.7	10.49	1.45	0.054
Glu	9.0	10.11	1.43	0.056
Thr	9.4	9.64	1.40	0.058
His(0) ^f	9.5	9.53	1.39	0.059
Met	10.0	9.00	1.36	0.062
Ser	10.3	8.71	1.35	0.064
Val	10.4	8.62	1.34	0.065
Gln	11.5	7.70	1.28	0.072
Asn	11.6	7.62	1.28	0.073
Leu	12.0	7.33	1.26	0.076
Ile	12.0	7.33	1.26	0.076
Gly	13.7	6.30	1.18	0.087
His(+) ^g	16.5	5.06	1.07	0.107
Phe	23.0	3.35	0.87	0.155
Tyr	24.0	3.20	0.85	0.163
Trp	37.7	1.65	0.58	0.280

^aReplicated from **Table 2** in Huyghues-Despointes et al. (12).

^bThe percentage of *cis* conformer measured at 23°C in 20 mM sodium phosphate at pH 6.0 (33). This value is relatively independent of temperature (38).

^cK_{Pro} is the equilibrium constant for *cis* ⇌ *trans* isomerization of the indicated Xaa-Pro residue.

^dCorrection in kcal/mol at 25°C (Eq. 10) for *cis* Xaa-Pro residues.

^eCorrection in kcal/mol at 25°C (Eq. 11) for *trans* Xaa-Pro residues.

^fMeasured at pH 8.0.

^gMeasured at pH 3.5.

isomerization (12). The protein typically spends less than 1 s in the transiently populated unfolded state before all the amide protons are exchanged. This is shown for the folding equilibrium of a protein with a proline residue in the sequence:



where F_{cis} and U_{cis} are the native and unfolded states with a Pro residue exclusively in the *cis* conformation. K_{pro}^U is the equilibrium constant for *cis/trans* proline isomerization in the unfolded state, and K_{HX} is the equilibrium constant for folding exclusively in the *cis* conformation. The denatured states will have a higher free energy in the hydrogen-exchange experiments than under the traditional unfolding experiments where the proline bonds reach *cis/trans* equilibrium. ΔG_{HX} measures ΔG for the first step in the equilibrium, but ΔG_U measures ΔG for both steps (15,34). The total difference is the stability from proline isomerization in the folded and unfolded states:

$$\Delta G_{pro} = \Delta G_{HX} - \Delta G_U = RT \ln(1 + K_{pro}^U)/(1 + K_{pro}^F) \quad (9)$$

The full expression (Eq. 9) must be used for proteins such as Staphylococcal nuclease (SNase) where two proline residues flip between *cis* and *trans* conformers in the folded state (see Table 2).

For most proteins, where the proline conformation is fixed in the native conformation, the stability from proline isomerization caused by a *cis* proline in the native state can be reduced to:

$$\Delta G_{pro}^U = RT \ln(1 + K_{pro}^U) \quad (10)$$

or using Eq. 8, a *trans* proline in the native state can be:

$$\Delta G_{pro}^U = RT \ln(1 + 1/K_{pro}^U) \quad (11)$$

The ΔG_{pro}^U values for a *cis* proline in the native state are more than 1 kcal/mol, while ΔG_{pro}^U for a *trans* proline are much smaller (< 0.3 kcal/mol). Table 3 shows the ΔG_{pro}^U values for *cis* and *trans* proline conformers at 25°C. The total effect of proline isomerization is determined by summing ΔG_{pro}^U contributions for all *cis* and *trans* proline residues in a protein. The conformation of a Xaa-Pro bond is detected by measuring the ω angle in the best NMR or X-ray crystal structure of a protein.

Until recently, it was commonly assumed that the proline bond was approx 20% *cis* in the unfolded state at equilibrium for all Xaa-Pro residues in a protein. As a result, the stabilities of the most stable residues were not always considered to exchange by global unfolding (*see refs. 35–37*), because these stabilities did not agree and were often higher than the values from traditional methods.

6. Conclusion

If the corrections for the proline isomerization of the Xaa-Pro bond using values of Reimer et al. (33) are applied and if the traditional experiments are performed in D₂O, we find an excellent agreement between the corrected ΔG_{HX} and ΔG_{U} for most proteins (Table 1). This comparison leads to several important conclusions:

1. The most stable amide hydrogens generally exchange by global unfolding.
2. The unfolded states that exist under native conditions are thermodynamically equivalent to those that exist after solvent or thermal unfolding.
3. Chemical exchange rates from short peptides can model well k_{rc} , the exchange-rate constant of the open conformation.
4. The equilibrium constants for proline isomerization in capped pentapeptides can be used to correct for the higher free energy of the unfolded states in the hydrogen-exchange experiments.

7. A Note on Nomenclature

In the literature, the nomenclature for describing the hydrogen-exchange process varies widely. Examples include defining the chemical exchange-rate constants as k_{rc} , k_{ch} , or k_{int} , the hydrogen-exchange stabilities as ΔG_{HX} , ΔG_{HD} , or ΔG_{ex} , the conformational stability as ΔG_{U} , ΔG_{W} , or $\Delta G(\text{H}_2\text{O})$, the hydrogen-exchange process as HX, HD, or hydrogen exchange, and the pH meter reading of the experiment in D₂O as pH*, pH_{read}, or pD. In this chapter, all these terms are defined as the following: the random coil rate as k_{rc} , the hydrogen exchange stabilities as ΔG_{HX} , the conformational sta-

bility in 0 M denaturant as $\Delta G_U(D_2O)$ in deuterated solvent and $\Delta G_U(H_2O)$ in protonated solvent, the exchange process as hydrogen-exchange or HX, and the pH meter reading as pH*. In the future, for the purpose of clarity, it would be advisable to universally adopt the same nomenclature, and we suggest that the nomenclature defined here would serve this purpose.

Acknowledgment

Work in the authors' laboratories is supported by the National Institutes of Health (J. M. Scholtz, C. N. Pace, and S. W. Englander) and the Robert E. Welch Foundation (J. M. Scholtz and C. N. Pace).

References

1. Pace, C. N., Shirley, B. A., McNutt, M., and Gajiwala, K. (1996) Forces contributing to the conformational stability of proteins. *FASEB J.* **76**, 75–83.
2. Pace, C. N. (1975) The stability of globular proteins. *CRC Crit. Rev. Biochem.* **3**, 1–43.
3. Freire, E. (1995) Thermal denaturation methods in the study of protein folding. *Methods Enzymol.* **259**, 144–168.
4. Pace, C. N. and Scholtz, J. M. (1997) Measuring the conformational stability of a protein, in *Protein Structure. A Practical Approach*, (Creighton, T. E., ed.), Oxford University Press Inc., New York, NY, pp. 299–321.
5. Jaenicke, R. (1987) Folding and association of proteins. *Prog. Biophys. Mol. Biol.* **49**, 117–237.
6. Makhatadze, G. I. (1999) Thermodynamics of protein interactions with urea and guanidinium hydrochloride. *J. Phys. Chem.* **103**, 4781–4785.
7. Chamberlain, A. K. and Marqusee, S. (1997) Touring the landscapes: partially folded proteins examined by hydrogen exchange. *Structure* **5**, 859–863.
8. Hvidt, A. and Neilson, S. O. (1966) Hydrogen exchange in proteins. *Adv. Protein Chem.* **21**, 287–386.
9. Bai, Y., Milne, J. S., Mayre, L., and Englander, S. W. (1993) Primary structure effects on peptide group hydrogen exchange. *Proteins* **17**, 75–86.

10. Loh, S. N., Rohl, C. A., Kiefhaber, T., and Baldwin, R. L. (1996) A general two-process model describes the hydrogen exchange behavior of RNase A in unfolding conditions. *Proc. Natl. Acad. Sci. USA* **93**, 1982–1987.
11. Qian, H. and Chan, S. I. (1999) Hydrogen exchange kinetics of proteins in denaturants: a generalized two-process model. *J. Mol. Biol.* **286**, 607–616.
12. Huyghes-Despointe, B. M. P., Scholtz, J. M., and Pace, C. N. (1999) Protein conformational stabilities can be determined from hydrogen-exchange rates. *Nat. Struct. Biol.* **6**, 910–912.
13. Connelly, G. P., Bai, Y., Jeng, M.-F., and Englander, S. W. (1993) Isotope effect in peptide group hydrogen exchange. *Proteins* **17**, 87–92.
14. Molday, R. S., Englander, S. W., and Kallen, R. G. (1972) Primary structure effects on peptide group hydrogen exchange. *Biochemistry* **11**, 150–158.
15. Bai, Y., Milne, J. S., Mayne, L., and Englander, S. W. (1994) Protein stability parameters measured by hydrogen exchange. *Proteins* **20**, 4–14.
16. Roder, H., Wagner, G., and Wüthrich, K. (1985) Amide proton exchange in proteins by EX1 kinetics: studies of the basic pancreatic trypsin inhibitor at variable pD and temperature. *Biochemistry* **24**, 7396–7407.
17. Tüchsen, E. and Woodward, C. (1987) *Biochemistry* **26**, 8073–8078.
18. Swint-Kruse, L. and Robertson, A. D. (1996) Temperature and pH dependences of hydrogen exchange and global stability for ovomucoid third domain. *Biochemistry* **35**, 171–180.
19. Mayo, S. L. and Baldwin, R. L. (1993) Guanidinium chloride induction of partial unfolding in amide proton exchange in RNase A. *Science* **262**, 873–876.
20. Bai, Y., Sosnick, T. R., Mayne, L., and Englander, S. W. (1995) Protein folding intermediates: native state hydrogen exchange. *Science* **269**, 192–197.
21. Chamberlain, A. K., Handel, T. M., and Marqusee, S. (1996) Detection of rare partially folded molecules in equilibrium with the native conformation of RNase H. *Nat. Struct. Biol.* **3**, 782–787.
22. Grantcharova, V. P. and Baker, D. (1997) Folding dynamics of the src SH3 domain. *Biochemistry* **36**, 15,685–15,692.
23. Yi, Q., Scalley, M. L., Simons, K. T., Gladwin, S. T., and Baker, D. (1997) Characterization of the free energy spectrum of peptostreptococcal protein L. *Fold. Des.* **2**, 271–279.

24. Bhuyan, A. K. and Udgaonkar, J. B. (1998) Two structural subdomains of barstar detected by rapid mixing NMR measurement of amide hydrogen exchange. *Proteins* **30**, 295–308.
25. Fuentes, E. J. and Wand, A. J. (1998) Dynamics and stability of apocytochrome b562 examined by hydrogen exchange. *Biochemistry* **37**, 3687–3698.
26. Fuentes, E. J. and Wand, A. J. (1998) Local stability and dynamics of apocytochrome B562 examined by the dependence of hydrogen exchange on hydrostatic Pressure. *Biochemistry* **37**, 9877–9883.
27. Huyghes-Despointe, B. M. P., Langhoest, U., Steyaert, J., Pace, C. N., and Scholtz, J. M. (1999) Hydrogen-exchange stabilities of RNase T1 and variants with buried and solvent-exposed Ala→Gly mutations in the helix. *Biochemistry*
28. Pace, C. N., Laurents, D. V., and Thomson, J. A. (1990) pH dependence of the urea and guanidine hydrochloride denaturation of ribonuclease A and ribonuclease T1. *Biochemistry* **29**, 2564–2572.
29. Glasoe, P. F. and Long, F. A. (1960) Use of glass electrodes to measure acidities in deuterium oxide. *J. Phys. Chem.* **64**, 188–193.
30. Oas, T. G. and Toone, E. J. (1997) Thermodynamic solvent isotope effects and molecular hydrophobicity, in *Adv. Biophys. Chem.* (Bush, C., ed.), JAI Press, Inc., Greenwich, CT pp. 1–52.
31. Makhatadze, G. I., Clore, G. M., and Gronenborn, A. M. (1995) Solvent isotope effect of protein stability. *Nat. Struct. Biol.* **2**, 852–855.
32. Jabs, A., Weiss, M. S., and Hilgenfeld, R. (1999) Non-proline *cis* peptide bonds in proteins. *J. Mol. Biol.* **286**, 291–304.
33. Reimer, U., Scherer, G., Drewello, M., Kruber, S., Schutkowski, M., and Fischer, G. (1998) Side-chain effects of peptidyl-prolyl *cis/trans* isomerization. *J. Mol. Biol.* **279**, 449–460.
34. Sharp, K. A. and Englander, S. W. (1994) How much is a stabilizing bond worth? *Trends Biochem. Sci.* **19**, 526–529.
35. Kragelund, B. B., Knudsen, J., and Poulsen, F. M. (1995) Local perturbations by ligand binding of hydrogen deuterium exchange kinetics in a four-helix bundle protein, acyl coenzyme A binding protein (ACBP). *J. Mol. Biol.* **250**, 695–706.
36. Li, R. and Woodward, C. (1999) Hydrogen exchange and protein folding. *Protein Sci.* **8**, 1571–1591.
37. Neira, J. L., Sevilla, P., Menéndez, M., Bruix, M., and Rico, M. (1999) Hydrogen exchange in ribonuclease A and ribonuclease S:

- evidence for residual structure in the unfolded state under native conditions. *J. Mol. Biol.* **285**, 627–643.
38. Sivaraman, T., Kumar, T. K. S., and Yu, C. (1999) Investigation of the structural stability of cardiotoxin analogue III from the taiwan cobra by hydrogen-deuterium exchange kinetics. *Biochemistry* **38**, 9899–9905.
 39. Chakshumathi, G., Ratnaparkhi, G. S., Madhu, P. K., and Varadarajan, R. (1999) Native-state hydrogen-exchange studies of a fragment complex can provide structural information about the isolated fragments. *Proc. Natl. Acad. Sci. USA* **96**, 7899–7904.
 40. Llinás, M., et al. (1999) The energetics of T4 lysozyme reveal a hierarchy of conformations. *Nat. Struct. Biol.* **6**, 1072–1076.
 41. Loh, S. N., Prehoda, K. E., Wang, J., and Markley, J. L. (1993) Hydrogen exchange in unligated and ligated staphylococcal nuclease. *Biochemistry* **32**, 11,022–11,028.
 42. Wrabl, J. and Shortle, D. (1999) A model of the changes in denatured state structure underlying m value effects in staphylococcal nuclease. *Nat. Struct. Biol.* **6**, 876–883.
 43. Brandts, J. F., Halvorson, H. R., and Brennan, M. (1975) Consideration of the possibility that the slow step in protein denaturation reactions is due to *cis-trans* isomerization of proline residues. *Biochemistry* **14**, 4953–4963.